Angular Dependence of the Spin Photocurrent in a Spin Light Emitting Diode

Xiaodi Xue, Wei Huang, Laipan Zhu, Yang Zhang, Yuan Lu, Yu Liu, Yonghai Chen, Zhanguo Wang

Article

Journal of
Nanoscience and Nanotechnology
Vol. 18, 7573–7577, 2018
www.aspbs.com/jnn

Angular Dependence of the Spin Photocurrent in a Spin Light Emitting Diode

Xiaodi Xue[1,3,†], Wei Huang[1,2,†], Laipan Zhu[1,5], Yang Zhang[1,2], Yuan Lu[4], Yu Liu[1,2,*], Yonghai Chen[1,2,*], and Zhanguo Wang[1,2]

[1] *Key Laboratory of Semiconductor Materials Science, Institute of Semiconductors, Chinese Academy of Sciences, Beijing Key Laboratory of Low Dimensional Semiconductor Materials and Devices, Beijing 100083, China*
[2] *College of Materials Science and Opto-Electronic Technology, University of Chinese Academy of Sciences, Beijing 100049, China*
[3] *Henan Key Laboratory of Photovoltaic Materials, Laboratory of Low-Dimensional Materials Science, School of Physics and Electronics, Henan University, Kaifeng 475004, China*
[4] *Institut Jean Lamour, UMR 7198, CNRS-Université de Lorraine, BP 239, 54506 Vandoeuvre, France*
[5] *Beijing Institute of Nanoenergy and Nanosystems, Chinese Academy of Sciences, Beijing 100083, China*

We study the photogenerated spin currents in a spin light emitting diode when the device is excited under circularly polarized light. The device is based on a $In_{0.1}Ga_{0.9}As$ quantum well embedded in a *p–i–n* junction. The spin filtering is performed owing to a Co–Fe–B/MgO electrode with out-of-plane magnetization. The helicity-dependent photocurrent is explored as a function of the incident and azimuth angles of the incoming light wave vector with respect to the magnetization direction of the ferromagnetic electrode. The results are interpreted as a simple phenomenological model described in the paper, which demonstrates it is an efficient way to detect the remanent < (remnant?) magnetic moment of the ferromagnetic electrode at room temperature.

Keywords: Spin-Polarized Photo-Current, Spin-Filter, Quantum Well, Spectra, Spin Injection.

1. INTRODUCTION

Spintronic devices based on spin-polarized electrons offer the promise of significant advances in device performance, in terms of speed, size, and power consumption.[1–3] Among spintronic devices, spin light emitting diode (spin-LED)[4] has been proved to be an efficient way to transfer a solid-state information stored within ferromagnetic materials into circularly polarized photons emitted via carrier-photon angular momentum conversion. Several advanced semiconductor technologies have been proposed. Potential devices ranging from memory element with optical readout and optical transport of spin information,[5] advanced optical switches,[6] circularly polarized single photon emitters for quantum cryptography[7] to chiral analysis[8] and 3-dimensional display screens[9] have been anticipated. By reversing the operation condition of spin-LED, one can also realize spin photodiode (spin-PD) function by illuminating the device with circular polarized light and detect spin-polarization of photocurrent to obtain the conversion efficiency. Several research groups have investigated the possibility of creating a spin-polarized photocurrent under circular polarized light in spin-LED structures.[10] The current can be measured even at room temperature, which provides not only a powerful way to investigate the potential mechanisms of the spin detection but also promising applications in spin detectors of circular polarized light.[11]

The spin-polarized photocurrents in spin-LEDs were mostly studied under external magnetic fields;[12] thus, it is hard to distinguish whether the spin-polarized photocurrent before being spin-filtered by the ferromagnetic contact is derived from the intrinsic spin-orbit coupling (SOC) due to the Rashba effect in the semiconductor[13] or the Zeeman splitting effect.[14] So the study of spin-polarized photocurrent under zero magnetic field might reveal the real generation mechanisms for the spin-polarized photocurrent. Besides, the previous studies of spin-polarized photocurrents in spin-LEDs were mostly carried out at fixed excitation wavelength,[15] so they could not investigate or eliminate the Stark effect[16] induced by external voltages

*Authors to whom correspondence should be addressed.
†These two authors contributed equally to this work.

for the corresponding energy levels; therefore, the physical mechanisms of the spin photocurrent with the variation of external voltage were remains unclear imprecise.

In this work, we found that the vertical illumination on the spin-LED structure with circularly polarized light at room temperature can generate spin-polarized photocurrent without the need of an external magnetic field. By employing a ferromagnetic out-of-plane magnetized CoFeB/MgO as a spin filter, which is also understood by establishing a physical model similar to tunneling magneto resistance structure.[17] We investigate the influence of the incident and azimuth angles of the incoming light wave vector in a systematical way, and establish a simple phenomenological model that the spin-polarized photocurrent as a function of the angle with respect to the remanent (remnant?) magnetic moment. Our results are in good agreement with the theory that allows us to find an efficient way to detect the remanent magnetic moment of the ferromagnetic electrode at room temperature.

2. EXPERIMENTAL DETAILS

2.1. Sample Preparation

The quantum well *p–i–n* structure and the tunnel barrier were grown by molecular beam epitaxy (MBE), while the ferromagnet contact was deposited by sputtering. The *p–i–n* structure has the following layers. A 500 nm *p*-GaAs:Be ($p = 2.17 \times 10^{19}$ cm^{-3}) buffer layer was initially deposited on (001) *p*-GaAs:Zn ($p = 2 \times 10^{19}$ cm^{-3}) substrate, followed by a 200 nm *p*-GaAs ($p = 2 \times 10^{18}$ cm^{-3}) layer. Then, 50 nm un-doped GaAs/10 nm un-doped $In_{0.1}Ga_{0.9}As$ QW/50 nm un-doped GaAs and a 50 nm *n*-GaAs:Si ($n = 1 \times 10^{16}$ cm^{-3}) cap layer were deposited in turn. The surface of the *p–i–n* structure was passivated with arsenic in the III–V MBE chamber and then transferred through the air into another MBE-sputtering interconnected system. The arsenic capping layer was first desorbed at 300 °C by monitoring *in situ* reflection high energy electron diffraction patterns in the MBE chamber, and after that a 2.5 nm MgO tunnelling barrier layer was grown at 250 °C. Then the sample was transferred to the sputtering chamber to grow 1.1 nm CoFeB ferromagnetic layer. Finally, 5 nm Ta was deposited to prevent oxidation.[18] The 300 μm diameter circular mesas were then processed using standard UV photolithography and etching techniques.

2.2. Measurement

A mode-locked Ti: Sapphire laser with a repetition rate of 80 MHz and a pulse width of 140 fs serves as the excitation source. The excitation wavelength is tuned from 850 nm to 1000 nm which covers the excitation energy of the E1-HH1 transition in the $In_{0.1}Ga_{0.9}As$ QW at 300 K, and the spot diameter and power of the laser are 2 mm and 0.2 mW, respectively. The incident light goes through a polarizer and a photo-elastic modulator (PEM) whose retardation is set to be 0.25 lambda to yield a modulated circularly polarized light with a fixed modulating frequency at 50 KHz (1f), and the spin-polarized photocurrent (ΔI) is first amplified by a current pre-amplifier and then collected by a lock-in amplifier with the reference frequency of 50 KHz. A chopper with a frequency at 220 Hz is applied to produce a polarization independent light, which is used to measure the common photo-induced direct current (I_{ph}) that is proportional to the total number of photo-induced electrons, and I_{ph} is also first amplified by a current pre-amplifier and then collected by a lock-in amplifier with the reference frequency of 220 Hz. In this work, we studied the azimuth angle and the incident angle dependence of the circular polarization.

3. RESULTS AND DISCUSSION

The sample structure is sketched in Figure 1(a). The optical microscopy images of the measured device are shown in Figures 1(b) and (c). The excitation wavelength was fixed at 930 nm which corresponded to the excitation energy of the E1-HH1 transition (the first valence sub-band of heavy holes to the first conduction sub-band) in the $In_{0.1}G_{0.9}As$ QW at 300 K.[19] In the inset of Figures 2(a) and 3(a), we show the schematic of illumination configurations. Here, we define θ as the angle between the incident light and the out-of-plane direction of the sample. We define α as the angle between

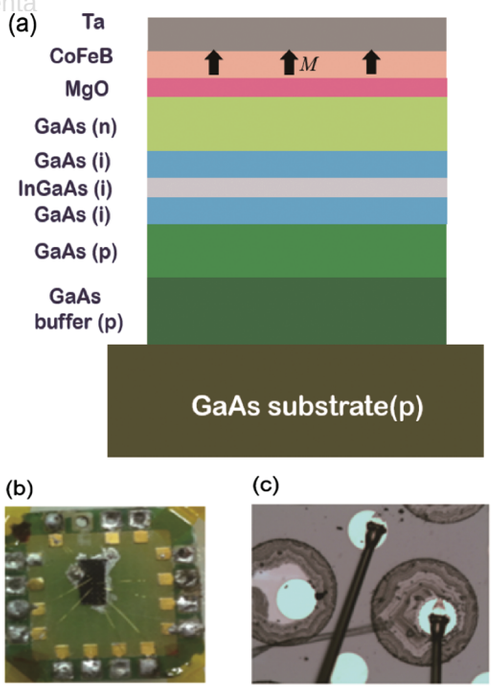

Figure 1. The structure of the sample. (a) The schematic diagram of the cross-section of the device. The black bold arrows denote the orientation of the remnant magnetic moment. (b) The images of the LED structure. (c) The optical microscopy images of the LED structure.

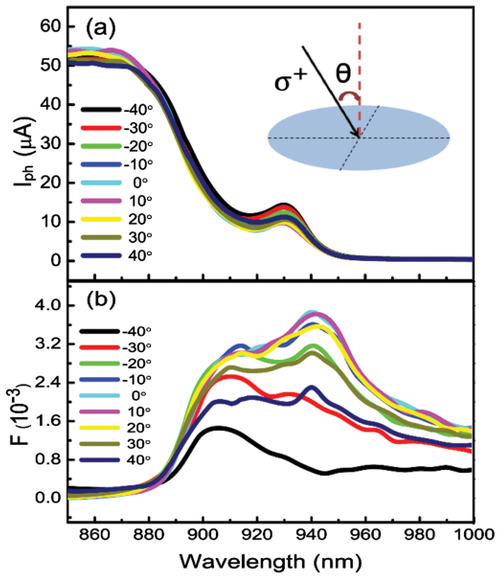

Figure 2. Incident angle dependence of the spectra of photocurrents and circular polarization at 300 K. (a) Spectra of the common photo-induced direct currents, (b) spectra of the circular polarization at different azimuth angle with the azimuth angle $\alpha = 0°$ under -0.1 V bias voltages at 300 K. The insets in (a) illustrate the definition of the incident angle.

the projection direction of the incident light and the preferred magnetic orientation is along [110] direction of the GaAs substrate. A photo-elastic modulator (PEM) with an intrinsic frequency of 50 KHz was employed to measure the helicity dependent photocurrent ΔI. The common photo-induced direct current I_{ph} was measured by an optical chopper with a rotation frequency of 220 Hz. Then the conversion efficiency (F) can be defined as $F = \Delta I / I_{ph}$, which contains the combination information of the light generated spin polarization in QW, the spin transport from QW to ferromagnetic layer/semiconductor interface and spin detection by the ferromagnetic layer.[20]

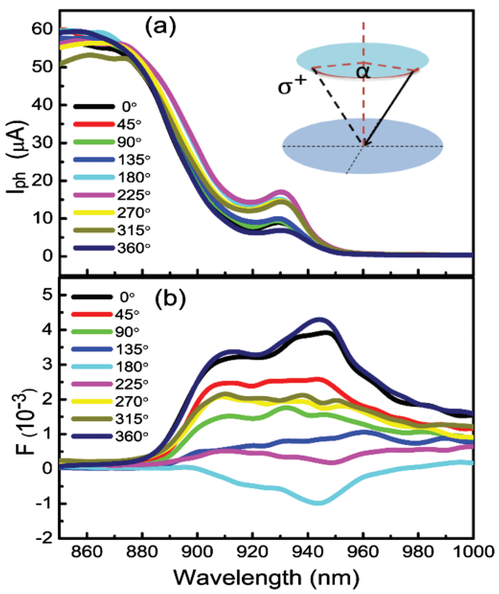

Figure 3. Azimuth angle dependence of the spectra of photocurrents and circular polarization at 300 K. (a) Spectra of the common photo-induced direct currents, (b) spectra of the circular polarization at different azimuth angle with the incident angle $\theta = 15°$ under -0.1 V bias voltages at 300 K. The insets in (a) illustrate the definition of the azimuth angle.

Figure 2(a) display the spectra of I_{ph} under different incident angle at 300 K, where $\alpha = 0°$. Figure 2(b) shows the deduced conversion efficiency with variation of light wavelength at different θ. We identified clearly the energy positions corresponding to the optical transitions in the i-$In_{0.1}Ga_{0.9}As$ QW at 930 nm. Figure 3(a) display the spectra of I_{ph} under different amzimuth angle at 300 K, where $\theta = 15°$. Figure 3(b) shows the deduced conversion efficiency with variation of light wavelength at different α.

Firstly, we studied the incident angle (θ) dependence of the photocurrent with the $\alpha = 0°$ of incident light at 300 K, as shown in Figures 4(a) and (b). The θ dependence of F shows a cosine-like behavior at -0.1 V bias voltages. From Figure 4(b) we can see that the maximal value of F is not completely at $\theta = 0°$. Secondly, we studied the excitation light azimuth angle dependence of the photocurrent with $\theta = 15°$ at 300 K, as shown in Figure 4(c). From 4(d) we can see that the azimuth angle α dependence of F also shows a cosine-like behavior at -0.1 V bias voltages. That F get maximal values when $\alpha = 0°, 360°$, while F almost vanishes and revises its sign when $\alpha = 180°$.

Since the direction of CoFeB magnetization is along out-of-plane direction, the variation F versus azimuth and incident angles could reflect the relative spin angle of electrons in the photocurrent. We can clearly find that the remanent magnetic moment of the ferromagnetic electrode at room temperature is not completely out-of-plane magnetized. Thus, we define φ as the angle between the remanent magnetic moment and the out-of-plane direction. When the vertical incident light irradiates on the surface of the sample, its out-of-plane component will, in accordance with conservation of angular momentum, induce polarized electrons with out-of-plane spin component which have the same direction as the one of the out-of-plane light component. Then these polarized electrons will move vertically towards the direction of ferromagnetic metal driven by the built-in internal electric field and the concentration gradient.[21] Ferromagnetic metal plays the exact role of spin filter,[22] enabling the spin-polarized electrons to pass easily when the spin polarization direction is parallel to the direction of ferromagnetic domains. However, the spin-polarized electrons with the direction anti-parallel to ferromagnetic domains can hardly pass the ferromagnetic metal. ΔI decrease its sign when in the direction of incident angle will result in different sign of the circular polarization.

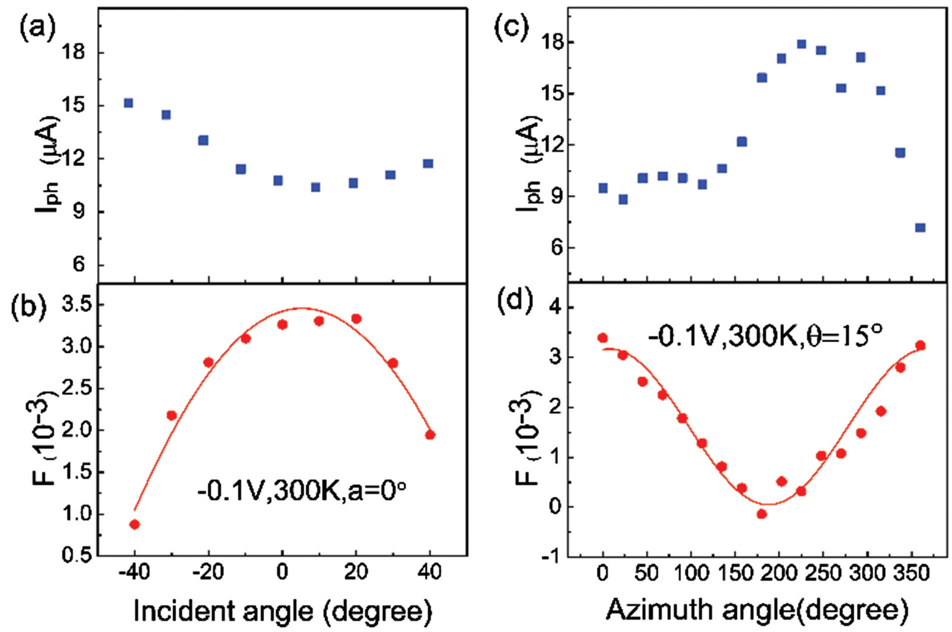

Figure 4. Photocurrents and circular polarization change with the azimuth angle and the incident angle. (a) The circular polarization as a function of the incident angle, (c) the circular polarization as a function of the azimuth angle, (b) the circular polarization as a function of the incident angle corresponding to the transition of $In_{0.1}Ga_{0.9}As$ QW, and (d) the circular polarization as a function of the incident angle corresponding to the transition of $In_{0.1}Ga_{0.9}As$ QW, the red line denoting a fitting line using Eq. (2).

For the in-plane magnetized electrode,[23] the equation is presented as

$$F = CP_{FM}\cos\alpha f(E_{Photon})\sin\theta \quad (1)$$

Where P_{FM} is the spin polarization of the ferromagnetic layer at the Fermi level, $f(E_{Photon})$ is a function that contains optical selection rules for electron-heavy-hole and electron-light-hole transitions in a QW.[24, 25] Because of the difference of the remanent magnetic moment, the relation between F and azimuth angle and incident angle can be empirically expressed as

$$F \propto \cos(\theta - \varphi)\cos\alpha \quad (2)$$

By employing the Eq. (2), he experimental dependence of F as a function of θ is in very good agreement with this model, as shown in Figure 4(b). The experimental dependence of F as a function of the azimuth angle α is also very well reproduced. The expected cosin (cosine?)-like behavior of F as a function of θ is indeed experimentally observed in Figure 4(d). Proved to be a very effective method to detect the remanent magnetic moment of the ferromagnetic electrode at room temperature.

4. CONCLUSIONS

In conclusion, we found a spin-polarized photocurrent in a spin-LED structure under different incident and azimuth angles without external magnetic field. The ferromagnetic metal CoFeB in the device could be regarded as a spin filter, hence an effective control of the transport of spin-polarized photocurrent was achieved. We find a very effective method to detect the remanent magnetic moment of the ferromagnetic electrode via employing different incident and azimuth angles.

Acknowledgments: This work was supported by the National Natural Science Foundation of China (Contract Nos. 11574302, 61474114, 11704032), the National Basic Research Program of China (Grant Nos. 2015CB921503, 2014CB643503 and 2013CB632805), National Key Research and Development Program (Grant Nos. 2016YFB0402303 and 2016YFB0400101).

References and Notes

1. G. A. Prinz, *Science* 282, 1660 (**1998**).
2. S. Wolf, D. Awschalom, R. Buhrman, J. Daughton, S. Von Molnar, M. Roukes, A. Y. Chtchelkanova, and D. Treger, *Science* 294, 1488 (**2001**).
3. I. Žutić, J. Fabian, and S. Das Sarma, *Rev. Mod. Phys.* 76, 323 (**2004**).
4. R. Fiederling, M. Keim, G. Reuscher, W. Ossau, G. Schmidt, A. Waag, and L. W. Molenkamp, *Nature* 402, 787 (**1999**).
5. R. Farshchi, M. Ramsteiner, J. Herfort, A. Tahraoui, and H. T. Grahn, *Appl. Phys. Lett.* 98, 162508 (**2011**).
6. M. Holub and P. Bhattacharya, *J. Phys. D: Appl. Phys.* 40, R179 (**2007**).
7. P. Asshoff, A. Merz, H. Kalt, and M. Hetterich, *Appl. Phys. Lett.* 98, 112106 (**2011**).
8. J. Xu, A. Lakhtakia, J. Liou, A. Chen, and I. J. Hodgkinson, *Opt. Commun.* 264, 235 (**2006**).
9. D. Y. Kim, *Korean Phys. Soc.* 49, S505 (**2006**).

10. P. Renucci, V. G. Truong, H. Jaffrès, L. Lombez, P. H. Binh, T. Amand, J. M. George, and X. Marie, *Phys. Rev. B* 82, 195317 (**2010**).
11. S. Hovel, N. C. Gerhardt, M. R. Hofmann, F. Y. Lo, D. Reuter, A. D. Wieck, E. Schuster, W. Keune, H. Wende, O. Petracic, and K. Westerholt, *Appl. Phys. Lett.* 92, 242102 (**2008**).
12. S. J. Steinmuller, C. M. Gürtler, G. Wastlbauer, and J. A. C. Bland, *Phys. Rev. B* 72, 045301 (**2005**).
13. S. Ganichev and W. Prettl, *Journal of Physics: Condensed Matter* 15, R935 (**2003**).
14. M. Oestreich and W. W. Rühle, *Phys. Rev. Lett.* 74, 2315 (**1995**).
15. A. F. Isakovic, D. M. Carr, J. Strand, B. D. Schultz, C. J. Palmstrøm, and P. A. Crowell, *Phys. Rev. B* 64, 161304 (**2001**).
16. H. Q. Le, J. J. Zayhowski, and W. D. Goodhue, *Appl. Phys. Lett.* 50, 1518 (**1987**).
17. Y. Lu, M. Tran, H. Jaffres, P. Seneor, C. Deranlot, F. Petroff, J. M. George, B. Lepine, S. Ababou, and G. Jezequel, *Phys. Rev. Lett.* 102, 4 (**2009**).
18. P. Barate, S. Liang, T. T. Zhang, J. Frougier, M. Vidal, P. Renucci, X. Devaux, B. Xu, H. Jaffres, J. M. George, X. Marie, M. Hehn, S. Mangin, Y. Zheng, T. Amand, B. Tao, X. F. Han, Z. Wang, and Y. Lu, *Appl. Phys. Lett.* 105, 012404 (**2014**).
19. J. L. Yu, Y. H. Chen, Y. Liu, C. Y. Jiang, H. Ma, L. P. Zhu, and X. D. Qin, *Appl. Phys. Lett.* 102, 5 (**2013**).
20. X. J. Wang, I. A. Buyanova, F. Zhao, D. Lagarde, A. Balocchi, X. Marie, C. W. Tu, J. C. Harmand, and W. M. Chen, *Nat. Mater.* 8, 198 (**2009**).
21. Q. Wu, Y. Liu, H. L. Wang, Y. Li, W. Huang, J. H. Zhao, and Y. H. Chen, *Sci. Rep.* 7, 8 (**2017**).
22. P. Renucci, V. G. Truong, H. Jaffres, L. Lombez, P. H. Binh, T. Amand, J. M. George, and X. Marie, *Phys. Rev. B* 82, 195317 (**2010**).
23. L. Zhu, W. Huang, P. Renucci, X. Marie, Y. Liu, Y. Li, Q. Wu, Y. Zhang, B. Xu, Y. Lu, and Y. Chen, *Phys. Rev. Appl.* 8, 064022 (**2017**).
24. A. M. Fox, D. A. B. Miller, G. Livescu, and J. E. Cunningham, *IEEE J. Quantum Electron.* 27, 2281 (**1991**).
25. X. Marie, T. Amand, J. Barrau, P. Renucci, P. Lejeune, and V. K. Kalevich, *Phys. Rev. B* 61, 11065 (**2000**).

Received: 1 February 2018. Accepted: 1 April 2018.